Functional and Biophysical Analysis of the C-Terminus of the CGRP-Receptor; a Family B GPCR[†]

Matthew Conner,[‡,§] Matthew R. Hicks,[§,||] Tim Dafforn,[‡] Timothy J. Knowles,[⊥] Christian Ludwig,[⊥] Susan Staddon,[#] Michael Overduin,[⊥] Ulrich L. Günther,[⊥] Johannes Thome,[▽] Mark Wheatley,[‡] David R. Poyner,[#] and Alex C. Conner*[,○]

School of Biosciences, University of Birmingham, Birmingham, B15 2TT, U.K., Department of Chemistry, Warwick University, Coventry, CV4 7AL, U.K., CRUK: Institute for Cancer Studies, University of Birmingham, Birmingham, U.K., School of Medicine, Institute of Life Science, Swansea University, Swansea SA2 8PP, U.K., School of Life and Health Sciences, Aston University, Birmingham, B4 7ET, U.K., and Warwick Medical School, Warwick University, Coventry, CV4 7AL, U.K.

Received March 10, 2008; Revised Manuscript Received May 28, 2008

ABSTRACT: G-protein coupled receptors (GPCRs) typically have a functionally important C-terminus which, in the largest subfamily (family A), includes a membrane-parallel eighth helix. Mutations of this region are associated with several diseases. There are few C-terminal studies on the family B GPCRs and no data supporting the existence of a similar eighth helix in this second major subfamily, which has little or no sequence homology to family A GPCRs. Here we show that the C-terminus of a family B GPCR (CLR) has a disparate region from N400 to C436 required for CGRP-mediated internalization, and a proximal region of twelve residues (from G388 to W399), in a similar position to the family A eighth helix, required for receptor localization at the cell surface. A combination of circular and linear dichroism, fluorescence and modified waterLOGSY NMR spectroscopy (SALMON) demonstrated that a peptide mimetic of this domain readily forms a membrane-parallel helix anchored to the liposome by an interfacial tryptophan residue. The study reveals two key functions held within the C-terminus of a family B GPCR and presents support for an eighth helical region with striking topological similarity to the nonhomologous family A receptor. This helix structure appears to be found in most other family B GPCRs.

G-protein coupled receptors (GPCRs) comprise one of the largest and most diverse mammalian superfamilies of proteins. They account for approximately 3% of the human genome, and around 40% of all commercially available drugs target one or more GPCRs (*1–3*). This makes the elucidation of the molecular structure and functional domains of these receptors crucial for understanding disease pathophysiology and designing therapeutic agents.[1]

The two major families of GPCRs (family A and B) share almost no significant sequence homology; however they both fold into a classic seven-transmembrane helical bundle. Family A GPCRs (the "rhodopsin-family") comprise the largest group. Their study has been greatly aided by the high definition crystal structure of the inactive state of rhodopsin (*4*), which has been used to construct homology models and guide mutagenic studies of other family A GPCRs (*5, 6*) as well as leading to the recent crystal structure of the β2-adrenergic receptor (*7*). The family B GPCRs comprise over fifteen distinct members with important roles in the recognition and response of peptides involved in metabolism, the stress response and regulation of the vasculature (*8*). There is no crystal structure for any family B member, and family A structures cannot be used as a direct platform for analysis due to low sequence homology.

The C-termini of family A GPCRs have been shown to be involved in a range of functions including G-protein coupling, cell-surface localization and agonist-driven desensitization (*9, 10*). Mutations within the intracellular tail of GPCRs have long been associated with a variety of disease states including nephrogenic diabetes and retinitis pigmentosa (*11, 12*). A key feature of the C-termini of family A GPCRs is the so-called "8th helix", which was first observed in the rhodopsin crystal structure (*4*). This helix is located immediately following the TM helical bundle, lying parallel to the membrane. Its existence in the cannabinoid CB1 receptor has been suggested by circular dichroism (CD) and NMR studies (*13*). There is evidence that the eighth helix acts as a conformational switch involved in the activation

[†] M.O. and T.J.K. were supported by BBSRC and EU (PRISM). M.R.H. was supported by EPSRC, Grant GR/T09224/01. M.C. was funded by the University of Birmingham VIP award.

* Address correspondence to Alex Conner, Warwick Medical School, Warwick University, Gibbet Hill Road, Coventry, CV4 7AL, U.K. Tel: 00442476528376. Fax: 00442476574637. E-mail: a.c.conner@warwick.ac.uk.

[‡] School of Biosciences, University of Birmingham.

[§] Authors contributed equally.

[||] Department of Chemistry, Warwick University.

[⊥] CRUK: Institute for Cancer Studies, University of Birmingham.

[#] Aston University.

[▽] Swansea University.

[○] Warwick Medical School, Warwick University.

[1] Abbreviations: GPCR, G-protein coupled receptor; TM, transmembrane helix; ICL, intracellular loop; RCP, receptor component protein; HA, hemagglutin; DMEM, Dulbecco's modified Eagle's medium; BSA, bovine serum albumin; TBS, Tris-buffered saline; ELISA, enzyme-linked immunosorbant assay; PBS, phosphate-buffered saline; MD, molecular dynamics; WT, wild type; rmsd, root mean squared deviation.

10.1021/bi8004126 CCC: $40.75
Published on Web 07/18/2008

of many GPCRs (*14–17*), and it modulates the expression of the rat melanin-concentrating hormone receptor 1 (*18*).

The C-termini of family-B GPCRs have been shown to have similar roles to those of family-A receptors. Studies have identified an interacting site for beta-arrestin 2 within the C-terminus of the glucagon-like peptide 2 receptor (*19*), a contribution to the internalization mechanism of the $VPAC_1$ receptor by the distal C-terminus (*20*) and a filamin interaction site on the distal C-terminus of the rabbit calcitonin receptor (*21*). However, there is no experimental evidence for an eighth helix in the family B GPCRs, and almost no members have a palmitoylation site, used as a membrane-anchor for the eighth helix of family A GPCRs.

In previous studies, we have investigated the function of the CGRP receptor (*22–24*). This is a family-B GPCR that couples predominantly to G_s. It is somewhat unusual in that it consists of a GPCR-like entity, calcitonin receptor-like receptor (CLR) as well as two accessory proteins, receptor activity modifying protein 1 (RAMP1) and receptor component protein (RCP). However, despite these features, the studies of its transmembrane domain and intracellular loops suggest that its activation shares many features with other family-B GPCRs.

This paper describes a targeted series of deletion constructs of the CLR C-terminus. The results show that the proximal 12 residue region (the putative eighth helix) is a key determinant for the localization or stability of the receptor at the cell surface. We have confirmed structural predictions that this forms a helix by circular dichroism of a peptide corresponding to this sequence. Linear dichroism, fluorescence studies and waterLOGSY NMR demonstate that the peptide lies parallel to the membrane where it is anchored via its tryptophan. We also demonstrate a significant role for a distal region of around fifty residues of the C-terminus in agonist-mediated cell surface internalization, with clear biological effects on the activation of intracellular MAPK.

EXPERIMENTAL PROCEDURES

Materials. Human αCGRP was from Calbiochem (Beeston, Nottingham, U.K.). The CLR eighth helix peptide (Acetyl-GEVQAILRRNWN-amide) was synthesized by Alta Bioscience (Birmingham, U.K.) using automated solid-phase F-moc chemistry. Peptides were dissolved in milliQ water (Millipore, Watford, U.K.) of resistivity 18.2 MΩ·cm and stored as aliquots at −20 °C in nonstick microcentrifuge tubes (Thermo Life Sciences, Basingstoke, U.K.). Unless otherwise specified, chemicals were from Sigma (Poole, Dorset, U.K.) or Fisher (Loughborough, U.K.). Cell culture reagents were from Gibco BRL (Paisley, Renfrewshire, U.K.) or Sigma.

Expression Constructs and Mutagenesis. Human CLR with an N-terminal hemagglutinin (HA) epitope tag (YPYDVPDYA) (*25*) was provided by Dr. S. M. Foord (GlaxoWellcome, Stevenage, U.K.) and was subcloned into pcDNA3(−) (Invitrogen, Renfrew, U.K.) prior to mutagenesis. Introduction of the epitope did not affect the pharmacology of the receptor (*25*). Mutagenesis was carried out using the Quick Change site-directed mutagensis kit (Stratagene, Cambridge, U.K.), following the manufacturer's instructions. Forward and reverse oligonucleotide primers were designed with single base changes to incorporate alanine point mutations in the final CL protein and to engineer restriction sites to aid screening of mutants. Deletions were created in exactly the same way incorporating two consecutive stop codons (TGA) after the desired terminal residue. The primers were synthesized by Invitrogen (U.K.). The numbering of the residues uses that adopted by SwissProt. The deletions in the coding sequence are shown (Figure 1). Plasmid DNA was extracted from the cultures using a Wizard-Prep DNA extraction kit according to the manufacturer's instructions (Promega, Southampton, U.K.). The plasmid DNA was eluted in 100 μL of sterile distilled water and stored at −20 °C. Sequences were confirmed by sequencing (Functional Genomics, Birmingham, U.K.).

Cell Culture and Transfection. Cos-7 cells were cultured in Dulbecco's modified Eagle's medium (DMEM) supplemented with 10% (v/v) fetal bovine serum and 5% (v/v) penicillin/streptomycin in a humidified 95% air/5% CO_2 atmosphere. For transfection, the cells were plated onto either 12 or 48 well plates. Cells were transfected using a mixture (per 1 μg of DNA) of 6 μL of 10 mM polyethyleneimine and 45 μL of 5% glucose solution incubated for 30 min at room temperature and added to an appropriate final volume of full media. Twelve and 48 well plates were treated with 1 μg of DNA per well. Characterization of expressed receptors was performed 48−72 h after transfection.

Assay of cAMP Production. Growth medium was removed from the cells and replaced with DMEM containing 500 μM isobutyl methyl xanthine for 30 min. αCGRP in the range 10 pM to 1 μM was added for a further 15 min. Ice-cold ethanol (95−100% v/v) was used to extract cAMP, which was subsequently measured by radio-receptor assay as previously described (*26*).

Analysis of Cell-Surface Expression of Mutants by Enzyme-Linked Immunosorbant Assay (ELISA). Cells in 12 well plates were transiently transfected with wild type (WT) or mutant HA-epitope tagged human CL and RAMP 1. The transfected cells were treated with 3.7% formaldehyde for 15 min after aspiration of growth medium. The cells were then washed three times with 0.5 mL of Tris-buffered saline (TBS). For permeabilized cells this was followed by a 30 min treatment with 0.1% Triton X-100 and three washes. Nonspecific binding of the antibody was blocked with 1% BSA in TBS for 45 min. The cells were treated with 250 μL of primary antibody (mouse, anti-HA antibody 12CA5 (Sigma-Aldrich, U.K.) diluted 1:1000 in TBS with 1% BSA) for 1 h, and the cells were washed again three times with 0.5 mL of TBS. A further block step was performed for 15 min before the cells were incubated with 250 μL of secondary antibody (anti-mouse, horseradish peroxidase conjugated, Sigma diluted 1:1000 in TBS) for 1 h. The cells were washed a further three times before development with OPD tablets (Bio-Rad, Hemel Hempstead, U.K.) according to the manufacturer's instructions. Reactions were terminated with 100 μL/well of 1 M H_2S0_4. The absorbance measured by the ELISA showed a linear dependence on the DNA concentration used in the transfection.

MAPK Activation. Cells were serum starved for 2 h prior to addition of 100 nM CGRP for the times indicated. ERK phosphorylation was examined by Western blotting using phospho-specific antibodies (Santa Cruz, sc-7383), as described previously (*27*). Protein content of samples was measured by the RCDC Protein Assay (BioRad) prior to

a)

```
hCLR_C-term          GEVQAILRRNWNQYKIQFG-----NSFSNSEALR------------SASYTVSTISDGPGYS-HD
hCTR_C-term          NEVQTTVKRQWAQFKIQWN---QRWGRRPSNRSAR----------AAAAAAEAGDIPIYICHQEPR
Porcine CTR          HEVQGALKRQWNQYQA------QRWAGRRSTRAAN---AAAATAAAAAALAETVEIPVYICHQEPR
hCRFR2_C-term        GEVRSAVRKRWHRW-----------QDHHSLRVP-----------MARAMSIPTSPTRISFH-S-
hCRFR1_C-term        SEVRSAIRKRWHRW-----------QDKHSIRAR-----------VARAMSIPTSPTRVSFH-S-
hGIPR_C-term         KEVQSEIRRGWHHCRLRRS----LGEEQRQLPER-----------AFRALPSGSGPGEVPTS-RG
hGlucR_C-term        KEVQSELRRRWHRWRLGKV----LWEERNTSNHR-----------ASSSPGHGPPSKELQFG-RG
hVIPR2_C-term        SEVQCELKRKWRSRCPTP-----SASR--DYR-V-----------CGSSFSRNGSEGALQFH-RV
hVIPR_C-term         GEVQAELRRKWRRWHLQG-----VLGWNPKYRHP-----------SGGSNGATCSTQVSMLT-R-
hGHRHR_C-term        QEVRTEISRKWHGHDP---------ELLPAWRTR-----------AKWTTPSRSAAKVLTSM-C-
hGLP2R_C-term        GEVKAELRKYWVRFLLARHSGCRACVLGKDFRFL-----------GKCPKKLSEGDGAEKLR-KL
hPTHR1_C-term        GEVQAEIKKSWSRWTLALDFKRKARSGSSSYSYGPMVSHTSVTNVGPRVGLGLPLSPRLLPTA-TT
hGLP1R_C-term        NEVQLEFRKSWERWRL----------EHLHIQRD-----------SSMKPLKCPTSSSSG-ATL
hSecR_C-term         GEVQLEVQKKWQQWHL-----------REFPLH-----------PVASFSNSTKASHLEQS-Q-
hPTHR2_C-term        GEVQAEVKKMWSRWNLSVD-----WKRTPPCGSRRCGSVLTTVTHSTSSQSQVAASTRMVLISGKA

hCLR_C-term          CPSEHLNGKSIHDIENVLLKPENLYN-------------------------------------
hCTR_C-term          NEPANNQGEESAEIIPLN---IIEQESSA-----------------------------------
Porcine CTR          EEPAGEEPVVEVEGVEVIAMEVLEQETSA-----------------------------------
hCRFR2_C-term        ---IKQTAAV-------------------------------------------------------
hCRFR1_C-term        ---IKQSTAV-------------------------------------------------------
hGIPR_C-term         ----LSSGTLPGPGNEASRELESYC----------------------------------------
hGlucR_C-term        GGSQDSSAETPLAGG-LPRLAESPF----------------------------------------
hVIPR2_C-term        --GSRAQSFLQTETSVI------------------------------------------------
hVIPR_C-term         SPGARRSSSFQAEVSLV------------------------------------------------
hGHRHR_C-term        ----------------------------------------------------------------
hGLP2R_C-term        QPSLNSGRLLHLAMRGLGELGAQPQQDHARWPRGSSLSECSEGDVTMANTMEEILEESEI-----
hPTHR1_C-term        NGHPQLPGHAKPGTPALETLETTPPAMAAPKDDGFLNGSCSGLDEEASGPERPPALLQEEWETVM
hGLP1R_C-term        AGSSMYTATCQASCS--------------------------------------------------
hSecR_C-term         -------GTCRTSII--------------------------------------------------
hPTHR2_C-term        AKIASRQPDSHITLPGYVWSNSEQDCLPHSFHEETKEDSGRQGDDILMEKPSRPMESNPDTEGCQ

hPTHR2_C-term        GETEDVL
```

b)

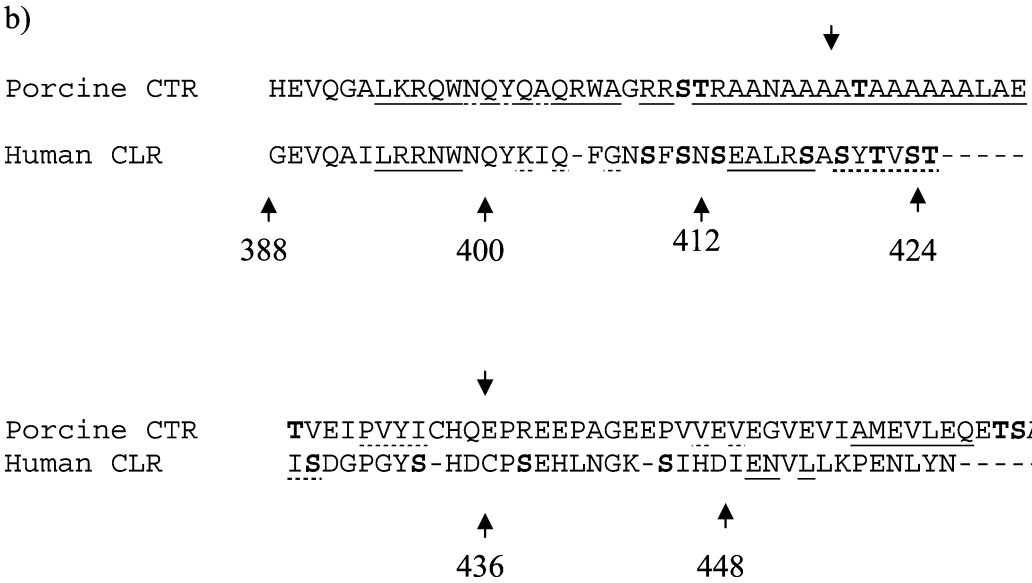

FIGURE 1: C-termini of family B GPCRs. (a) Comparison of human family B GPCRs, showing alignments and predicted structural features; the porcine calcitonin receptor is also included. Residues in bold are those in the 8th helix, those with solid underlining are predicted as α-helix and those in broken underlining are predicted as *β*-sheet. (b) Comparison of the C-termini of human CLR and porcine CTR. Shading shows conservation with human CLR. Arrows indicate deletions made for CLR in the current study and for CTR in ref *42*. Potential phosphorylation sites are in bold, those with solid underlining are predicted as α-helix and those in broken underlining are predicted as *β*-sheet.

Western blotting, to ensure equal loading. Blots were quantified by densitometry.

Liposome Preparation. Liposomes were prepared by dissolving L-α-phosphatidylcholine from Soybean (Sigma-

Aldrich, U.K.) in chloroform (99.8%) (Sigma-Aldrich, U.K.) and evaporating the chloroform under nitrogen to produce a thin film in a glass vial. After several hours under vacuum to remove residual chloroform, the lipid film was resuspended in water. The aqueous suspension of lipid was sonicated five times in a FB11021 sonicating water bath (Fisher Scientific U.K. Ltd., Loughborough, U.K.) for 30 s each time.

Circular Dichroism (CD). CD spectra of the putative eighth helix peptide from CLR (and a predicted nonhelical control; sequence: TGLGGGFPPLSSPQKASPQPMGGG-WQQGGGYNWQQTQ) in the presence of aqueous solutions of 2,2,2 trifluoroethanol (TFE) (Sigma-Aldrich, U.K.) and in the presence of liposomes were measured using a Jasco J715 spectropolarimeter (Jasco, Great Dunmow, U.K.). The cuvettes were supplied by Starna/Optiglass (Hainault, U.K.) and were 1 mm path length made from Spectrosil. Peptide concentration was 0.1 mg·mL^{-1}. Spectra were recorded from 260 to 180 nm with a bandwidth of 2 nm, a data pitch of 0.2 nm and a scan speed of 100 nm·min^{-1}. The response time was 0.5, and 8 spectra were averaged for each sample. Appropriate buffer baseline spectra were subtracted from each of the sample spectra. Spectra were truncated at low wavelength where the high voltage of the detector indicated that the signal was no longer linear with concentration. Percentage α-helix was calculated from the signal at 208 nm (*28, 29*).

Linear Dichroism (LD). LD spectra of the putative eighth helix peptide from CLR (and a predicted minimum hydrophobic moment, noninteracting control; sequence: GH-DQLVFLQSCP) in the presence of liposomes were measured using a Jasco J715 spectropolarimeter adapted for LD spectroscopy (Jasco, Great Dunmow, U.K.). The aligment of the samples was achieved using an ultra-low-volume linear dichroism accessory (Crystal Precision Optics, Rugby, U.K.) with a rotation speed of 4000 rpm. The path length of the cell was 0.5 mm, the peptide concentration was 0.5 mg·mL^{-1} and the lipid concentration was 7.5 mg·mL^{-1}. Spectra were recorded from 300 to 200 nm with a bandwidth of 2 nm, a data pitch of 0.2 nm and a scan speed of 100 nm·min^{-1}. The response time was 0.5, and 4 spectra were averaged for each sample. Spectra of the nonaligned (nonrotating) sample were subtracted from each of the spectra. Spectra were truncated at low wavelength where the high voltage of the detector indicated that the signal was no longer linear with concentration. Data were smoothed using the binomial algorithm in the Jasco spectral analysis program (Jasco, Great Dunmow, U.K.), paying attention not to distort the spectral shape.

Fluorescence. Fluorescence emission spectra were measured using a Perkin-Elmer LS50B luminescence spectrometer (Perkin-Elmer, Beaconsfield, U.K.). Excitation wavelength was 280 nm, and the emission was scanned at 100 nm·min^{-1} with both excitation and emission slits set to 2.5 nm. Spectra were measured in a 3 mm path length cuvette (Starna/Optiglass, Hainault, U.K.), type 16.45-F.

WaterLOGSY-NMR (SALMON) Experiments. 1 mM CLR eighth helix peptide was prepared in 50 mM sodium phosphate buffer pH 7.2 and 9:1 H_2O:D_2O. Soya bean lecithin (Sigma, U.K.) was prepared as a stock (20 mg/mL) in the same buffer and sonicated to produce ~50 nm phosphotidylcholine single unilamellar vesicles (PC SUVs). NMR was performed using the waterLOGSY NMR pulse sequence (*30*) using a novel data interpretation approach (*37*) on an 800 MHz Varian Inova Spectrometer equipped with cold probe technology at 25 °C on the eighth helix peptide with the following titrations of soya bean lecithin: 0, 0.01, 0.02, 0.04, 0.06, 0.10. 0.2, 0.4, 0.5 mg/mL. Data were collected using a spectral width of 12500 Hz, 16384 points, 32 scans and an NOE mixing time of 1 s (*31*).

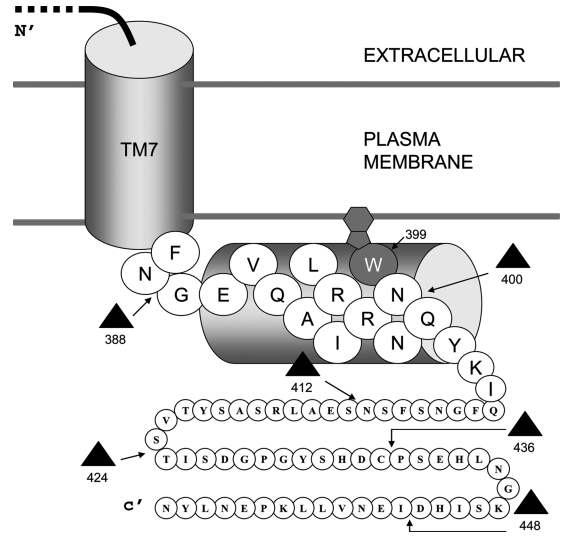

FIGURE 2: Schematic diagram of the intracellular C-terminus of CLR. Triangles indicate the deletion sites targeted in the study. The membrane-parallel orientation of the helix 8 region is shown, mediated by a flexible proximal glycine residue with the distal W399 inserted into the membrane.

Secondary Structure Analysis. Secondary structure prediction for the C-terminus of CLR was done using PELE from Biology Workbench 3.2 (http://workbench.sdsc.edu/). Hydrophobic moment analysis was done using MPEX (*32*).

Data Analysis. Curve fitting was performed with PRISM Graphpad 4 (Graphpad Software Inc., San Diego, CA). The data from each concentration−response curve were fitted to a sigmoidal concentration−response curve to obtain the maximum response and −log EC_{50} (pEC_{50}). pEC_{50} values were compared by paired Student's *t* test. Comparisons were only made between wild-type (WT) and mutant data from concomitantly transfected cells. A control WT experiment was always performed alongside a mutant experiment.

RESULTS

Effect of Deletions of the CLR C-Terminus on Coupling to G_s. To investigate the role of the C-terminus, a series of progressive deletions were prepared (outlined in Figure 2). There was no significant deleterious effect of either of the most extensive deletions (Del 388 and Del 400) on coupling to G_s as assessed by the CGRP-mediated cAMP response. pEC_{50} values were 9.85 ± 0.74 (n = 3) for wild type compared with 10.14 ± 0.56 (n = 3) for Del 388 and 10.33 ± 0.10 (n = 3) for wild type compared with 10.51 ± 0.15 (n = 3) for Del 400 (Figure 3). The basal and maximum levels of stimulation for Del 388 were not significantly different from those of the wild-type receptor (basal −29.8 ± 35.5% of WT; Emax 118.1 ± 23.5% of WT). For Del 400, although there was no change in the maximum, there was a small increase in basal cAMP production (basal −18.1 ± 3.4% of WT; Emax 105.1 ± 2.7% of WT). In light of

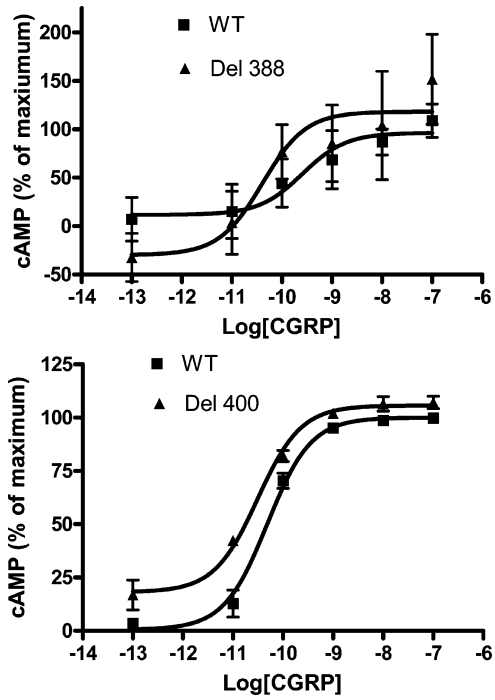

FIGURE 3: CGRP-stimulated cAMP response of the ICL2 mutants. Cos-7 cells were transfected with WT/RAMP1 or mutant/RAMP1 and assayed for CGRP-stimulated cAMP production. Squares: WT type receptors. Triangles: Mutant receptors. Data are the mean ± SEM of triplicate experiments.

Table 1: Expression and CGRP-Mediated Internalization of Deletion/Mutant Receptors[a]

mutant	surface expression % ± SE	internalization % ± SE	total serine/threonines
WT	100 (normalized)	70.12 ± 2.57	12
Del 388	10.16 ± 3.46**	13.80 ± 3.97**	0
Del 400	119.84 ± 9.78*	13.76 ± 2.61**	0
Del 412	91.21 ± 7.50	27.43 ± 0.77**	2
Del 424	99.28 ± 12.15	58.59 ± 1.27*	7
Del 436	101.60 ± 10.38	64.10 ± 2.89	10
Del 448	99.75 ± 8.83	69.62 ± 2.00	12
W399A	80.67 ± 30.12	76.76 ± 3.25	12
W399DEL	88.75 ± 3.49	63.45 ± 3.14	12
W399T	60.57 ± 5.50*	68.08 ± 5.64	13
W399E	14.10 ± 10.47**	83.10 ± 51.6	12

[a] Values are mean ± SEM of 3 to 5 determinations. Ab_{max}: relative cell surface expression of receptors as measured by detection of HA tags in an ELISA. Data normalized to WT as 100%. Significant difference between values measured using Student's *t* test and compared with WT is indicated (*P < 0.05%; **P < 0.001%). Also shown are the total serine/threonine residues found in the C-terminus of each deletion.

this data, the less extensive deletions were not examined for G_s coupling.

Effect of the Deletions on Expression and Internalization of CLR. Interestingly, ELISA data showed that Del 388 had an extremely limited surface expression at the plasma membrane of approximately 10% of wild-type surface localization, while total cellular expression (using triton-permeabilized cells) did not significantly differ (Table 1). Additionally, the CGRP-mediated internalization of those mutant receptors which did traffic to the surface was almost completely impaired compared with wild-type (Table 1).

ELISA data for the second deletion (Del 400) removing the remaining 61 C-terminal residues showed a slight overexpression compared with wild-type in marked contrast to the reduction in expression seen for the Del 388 mutant

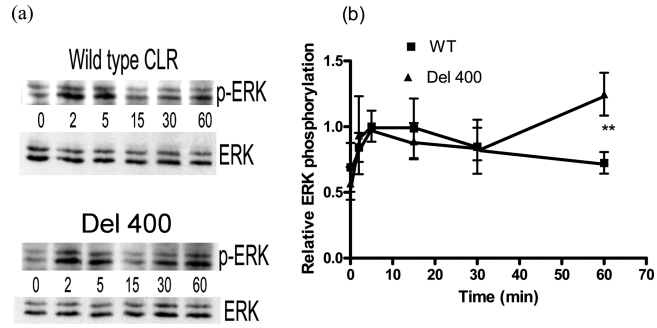

FIGURE 4: MAPK activation profile of WT and DEL 400. Deletion of the C terminus caused sustained phosphorylation of ERK. (a) Cells were stimulated with CGRP for the times indicated (min) and probed with antiphospho-ERK IgG (p-ERK) or anti-ERK IgG (ERK). Result shown is a representative blot. (b) Bands were quantified by densitometry and expressed as % maximum phosphorylation. Results are expressed as mean ± SEM for 5 individual experiments. **P < 0.01 vs WT.

(Table 1). Unlike the surface expression, the CGRP-mediated internalization of Del 400 was not recovered (Table 1). These data show that one or more of the residues between 388 and 400 are crucial for cell-surface expression of the receptor but that residues further downstream are required for agonist-mediated internalization. To assess the internalization further, a nested series of C-terminal deletions was constructed and analyzed for CGRP-mediated internalization and cell-surface localization. These effectively led to the sequential addition of 12 amino acids at a time creating four further deletion constructs: Del 412, Del 424, Del 436 and Del 448 (Figure 1). These data (Table 1) showed around 25% recovery of internalization for Del 412, 80% recovery for Del 424 and almost full restoration for Del 436 and 448. This shows that the bulk of the effect was predominantly within the region between 412 and 424 although with important contributions from the flanking regions.

CGRP MAPK Activation Is Enhanced by the Internalization-Deficient Mutant Del 400. CGRP stimulates phosphorylation of ERK1/2 in transfected Cos 7 cells (Figure 4); as this is reduced by 82 ± 7% (n = 4) by 1 μM wortmannin, the stimulation is likely to be predominantly by phosphatidylinositol-3-kinase. To examine whether the decreased internalization had any functional correlate, the ability of Del 400 to stimulate MAPK was examined. It was able to produce a normal acute CGRP-mediated stimulation of ERK1/2 phosphorylation; however, this response was sustained at 60 min compared to WT (Figure 4: 125 ± 16% versus 72 ± 8%, n = 5, P < 0.01, Mann−Whitney). Total ERK expression remained unchanged.

Secondary Structure of the C-Terminus. To assess the potential for secondary structure formation within the C-terminus of CLR, a consensus of seven secondary structure predictors was taken using the PELE alogarithim (Figure 1). Furthermore, the comparison was extended across the C-termini of the main human family-B GPCRs. Analysis of primary structure confirmed that there is very little sequence conservation across the family, but what there is is found at the proximal end of the C-terminus. The equivalent of E389, V390 and W399 are absolutely conserved, and there is homology with other residues, leading to a consensus sequence of E-V-R/Q-x-x-hydrophobic-hydrophilic (usually basic)-R/K-x-W-N. The analysis of secondary structure

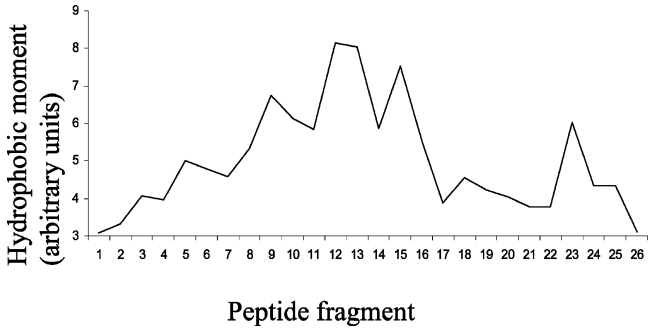

FIGURE 5: Hydrophobic moment plots of 26 sequential 11 amino acid segments from the top of TM7 (Q330) to the region distal of the last predicted residue of putative 8th helix. There is a clear peak of hydrophobicity in the 12th and 13th sequences corresponding to the putative 8th helix from residues G387 to N400.

indicated that, in every receptor, this has at least some propensity to form an α-helix. This is the region of helix 8 in family-A GPCRs.

Within CLR, there were other regions of predicted structure. Beyond the putative helix 8 (shown in Figure 2), there were suggestions of a β-sheet extending the ordered domain to G407. There was another region of potential structure with a short α-helix and a β-sheet between E414 and T425. Finally, at the extreme C-terminus, there was a predicted α-helix beginning at E450. Across all 14 receptors, 12 had evidence of a second structural domain within twenty or so amino acids of the putative eighth helix and 7 had suggestions of a structured domain close to their extreme C-termini.

The individual secondary structure alogarithims predicted that helix 8 in CLR could span five to twelve amino acids. To further delineate this structure the local hydrophobicity was investigated using hydrophobic moment analyses. Generally, an optimal sequence window for amphipathic helix formation consists of approximately eleven residues (*33, 34*). Each eleven-residue sequence starting from the glutamine residue (Q376) at the beginning of TM7 was measured for their hydrophobic moment (Figure 5). The boundaries were identified previously by TM boundary calculations (*23, 24*). There was a clear peak in potential amphipathic helix formation seen for 11−12 residues immediately following TM7 at G387, consistent with the presence of an eighth helix. Additionally hydrophobic moment values were calculated in the same way for each of the TM helices and hydrophilic loops from the CGRP-receptor and compared with the putative eighth helix. The putative eighth helix region had a hydrophobic moment (8.04) in excess of that seen for any of the extracellular or intracellular (usually less-helical) regions (0.88−5.51) and was comparable to the helical transmembrane domains (2.71−18.5).

Helical Structure Determined by Circular Dichroism (CD). To determine whether the proximal C-terminus could form a helix, a peptide with its amino acid sequence was synthesized and analyzed using CD spectroscopy.

CD is the difference in absorbance of left-handed and right-handed circular polarized light. For peptides, the resulting spectrum indicates the secondary structure. For example a spectrum from an α-helix will have a maximum at 192 nm and two minima at 208 and 222 nm. Unfolded peptides will have a single minimum of around 205 nm.

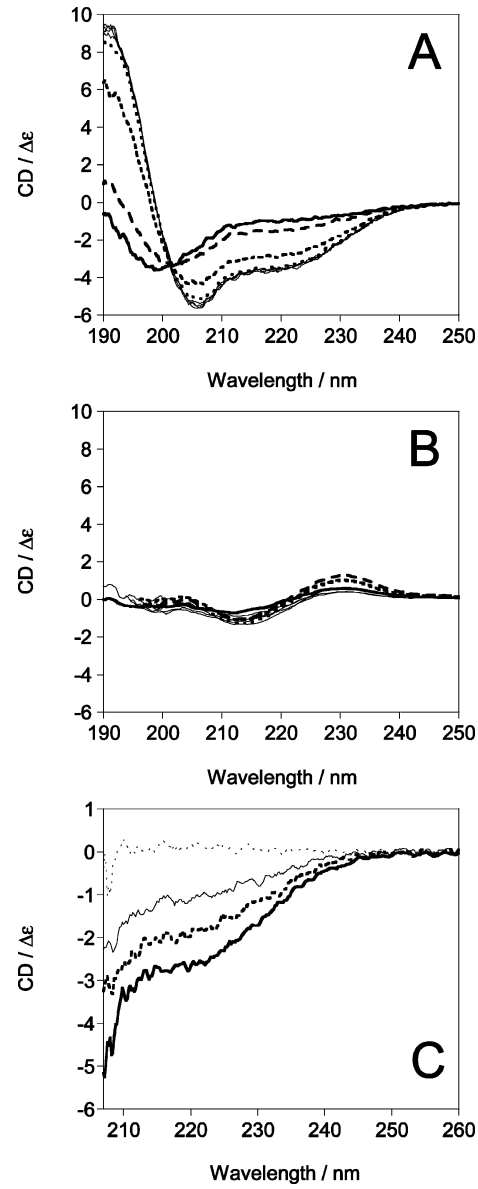

FIGURE 6: CD spectra of the 8th helix peptide (A) and nonhelical control peptide (B) in different concentrations of TFE: 0% (thick line, solid line), 10% (thick line, long dashes), 20% (thick line, medium dashes), 30% (thick line, short dashes), 40%, 50%, 60% and 70% (thin solid lines). (C) CD spectra of 2 mg·mL^{-1} lipid (thin line, dashed) and the 8th helix peptide in the presence of water (thin line, solid), 1 mg·mL^{-1} lipid (thick line, dashed) and 2 mg·mL^{-1} lipid (thick line, solid).

Furthermore, the magnitude of the signal correlates with the percentage of secondary structure present.

In the presence of the helix-inducing agent TFE (Figure 6A), spectra typical for α-helices were observed, with maxima around 190 nm (192 nm for 100% α-helix), minima around 206 nm (208 nm for 100% α-helix) and a shoulder around 222 nm (where there is a minimum for 100% α-helix). In the absence of TFE, the peptide showed 16% α-helix. This increased to a maximum of 40−43% at TFE concentrations <30%. This is close to the theoretical maximum helix content for a 12-mer peptide, as the ends of peptides cannot form fully helical structures due to lack of hydrogen-bonding partners. The formation of α-helical structure at low concentrations of TFE indicates that this peptide has a high helical propensity (*35*). Conversely, a control peptide without such α-helical propensity showed

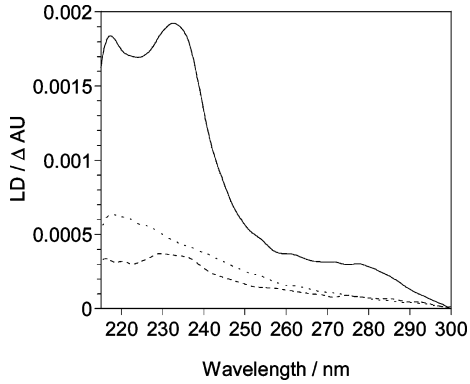

FIGURE 7: Linear dichroism spectra of phosphatidylcholine liposomes (7.5 mg/mL) (long-dashed line) and upon addition of CLR-8th helix peptide (0.5 mg/mL) (solid line). Liposomes with added control peptide (0.5 mg/mL) with minimum predicted hydrophobic moment (and therefore minimum predicted membrane association) are shown in the short-dashed line.

no significant increase in α-helix with TFE concentration (Figure 6B).

To investigate whether the eighth helix peptide formed α-helical structure in the presence of lipids, the CD spectrum was measured upon addition of liposomes composed of phosphatidylcholine, the most abundant lipid in the inner leaflet of the outer membrane. The spectra presented in Figure 6C are truncated at 207 nm because light scattering and turbidity in the sample caused by the liposomes rendered the data unreliable below this wavelength. Using a value of −12 for the $\Delta\epsilon$ value for 100% α-helix at 208 nm (*28, 29*), the peptide in water alone, in 1 $mg \cdot mL^{-1}$ lipid and in 2 $mg \cdot mL^{-1}$ lipid had respectively 17%, 27% and 36% % α-helix. This demonstrates a lipid concentration dependence of helix formation and thus an interaction between the peptide and the lipid.

Parallel Membrane Orientation Revealed by Linear Dichroism (LD). In this method, the liposomes are aligned by shear flow in the annular gap between a central stationary rod and a rotating outer cylinder. If the peptide is bound to the membrane in a particular orientation, the sign of the signal of different absorbance bands indicates the average orientation of the peptide relative to the membrane (*36, 37*). Note that a peptide not bound to the membrane will be isotropically oriented and will therefore give no difference in absorbance of the two polarizations of light (i.e., no LD signal). The LD signal around 280 nm is due to the tryptophan side chain in the peptide, as is the strong signal around 232 nm (Figure 7). For α-helices, there are 3 transitions in the far UV region (like in CD); the peptide backbone LD signals at 223 nm, 217 nm and <210 nm were assigned to the n to π^*, π to π^* (low energy) and π to π^* (high energy) transitions, respectively. Since LD is the difference in absorbance of light polarized parallel and perpendicular to the alignment axis, a different sign signal is obtained for an α-helix oriented on the membrane surface or inserted in the membrane (Figure 8). The LD signals observed here indicate a clear association with the membrane and show that the eighth helix peptide is lying on the membrane surface (i.e., as shown in the left-hand side of Figure 8). Furthermore, it was observed that a control peptide gave no LD signal under the same conditions (Figure 7).

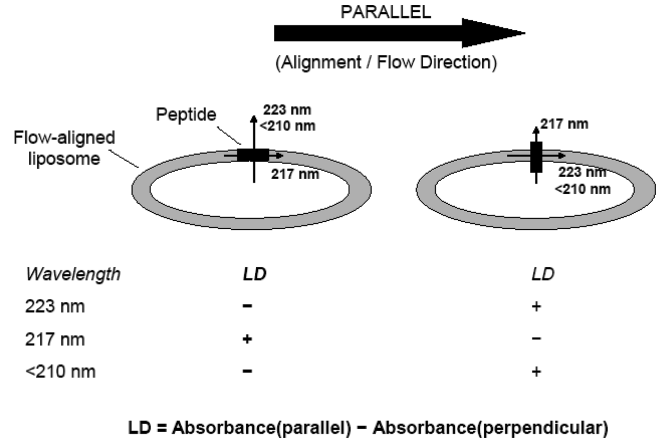

FIGURE 8: Schematic showing LD of membrane associated peptides. The large arrow indicates the alignment axis (this is the flow direction in the LD cell) and is denoted the parallel direction. The orientations of the peptide backbone transition moments and their wavelengths are illustrated by small arrows and the wavelength in nm. In the lower part of the figure the sign of the LD signal for the two different helix orientations is shown. Note that the left-hand side is the situation that we observe with the 8th helix peptide.

Tryptophan Interaction Mapped by WaterLOGSY NMR (SALMON) Spectroscopy. The bilayer interaction of the peptide corresponding to the CLR eighth helix was investigated using a new modified waterLOGSY NMR method (*31*). In this SALMON experiment (solvent accessibility, ligand binding and mapping of ligand orientation by NMR spectroscopy), bulk water magnetization is selected and transferred to the protein via both the nuclear Overhauser effect (NOE) and chemical exchange. The magnetization is then transferred to the ligand by a number of relay pathways before detection. The result shows two populations of signals, those with negative NOEs for ligands which bind to the protein, and those with positive NOEs for small molecules which do not. As the eighth helix peptide was of sufficiently small size to exhibit a positive NOE with bulk water alone, the technique could be used to study its interaction with the slower tumbling small unilamellar vesicles (SUVs) composed of phosphatidylcholine from soybean lecithin. Attention was directed to the tryptophan indole ring because of its well-resolved position in the proton spectrum avoiding the heavily overlapped aliphatic region (Figure 9).

Prior to SUV addition, all protons of the indole ring except H2 showed signals with a negative sign (positive NOEs) (Figure 9), confirming that the eighth helix was tumbling sufficiently fast and in contact with bulk water. The positive signal for H2 is presumably the result of its close proximity to the exchangeable amide proton at the H1 position resulting in NOE transfer. As all exchangeable protons gave positive signals (apparent negative NOE), the result is that H2 is positive. Following titration with liposome the signs of H4 and H7 invert, while H2 increases in intensity and H5 and H6 remain unchanged. The sign change for H4 and H7 show that these protons interact with the SUV and that interactions with bulk water are precluded. This is further confirmed by the increase in intensity for the H2 proton, showing that a further negative NOE contribution is occurring as a result of its interaction with the lipid. These results therefore confirm that the tryptophan of the eighth helix is interacting with the lipid. The distribution of NOE enhancements suggests an orientation of the tryptophan side chain such that

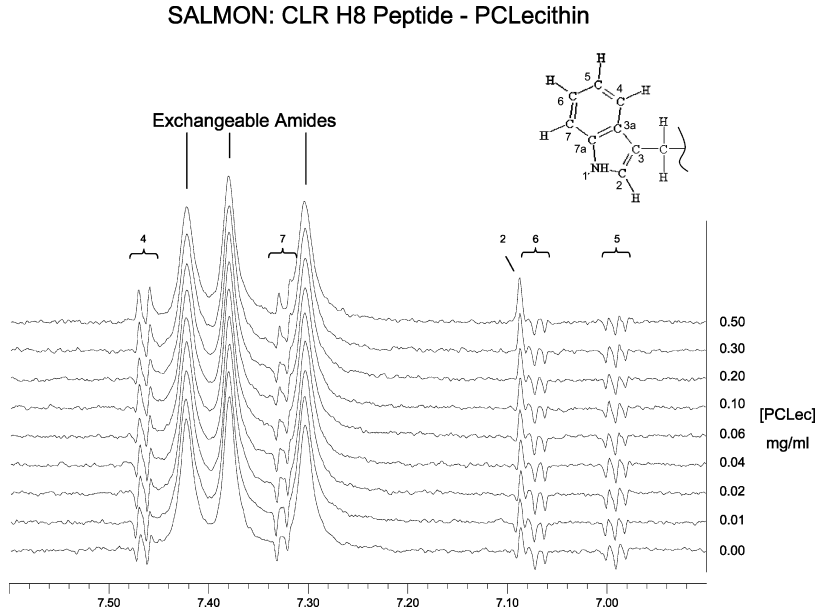

FIGURE 9: WaterLOGSY (SALMON) NMR spectra showing the NOE transfer of protons within the distal tryptophan of the synthetic 8th helix peptide in response to increasing PC lecithin. Signals from aromatic ring protons 4 and 7 change from negative to positive intensity suggesting lipid interaction.

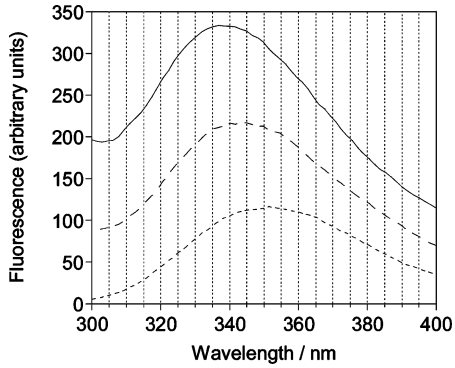

FIGURE 10: Fluorescence emission spectra of CLR-8th helix peptide (0.1 mg/mL) in water (short dashed line) and with phosphatidylcholine liposomes at 1 mg/mL (long dashed line) and 2 mg/mL (solid line).

the majority of the indole group is buried in the membrane with only the aromatic moiety being partially exposed. Such an orientation is possible if the backbone of the eighth helix is lying horizontally but partially inserted into the plane of the membrane.

Tryptophan Exposure in a Lipid Environment Measured by Fluorescence. The fluorescence emission spectrum of tryptophan residues is sensitive to the environment. Typically, if the tryptophan is exposed to aqueous solvent, the emission maximum will be around 350 nm. However, if the tryptophan is buried in a nonpolar environment, for example in the hydrophobic core of a protein or in a lipid membrane, the emission maximum will occur at a lower wavelength (usually around 330 nm) (*38*). Figure 10 shows clearly that the peak of the emission spectrum of the eighth helix peptide in water is approximately 350 nm, indicating that the tryptophan is exposed to the solvent and not buried. Upon addition of lipid membranes, the maximum shifts to a lower wavelength (around 345 and 340 nm for 1 mg·mL^{-1} and 2 mg·mL^{-1} lipid, respectively). This demonstrates that the tryptophan interacts with the membrane but is not totally buried in the hydrophobic part of the lipid bilayer. This is consistent with the NMR data which shows a partially buried tryptophan.

Functional Role of W399. Given the biophysical data suggesting an important role for W399 (illustrated in Figure 2), the functional properties of the mutant W399A were examined (Table 1). Substitution of the tryptophan by alanine did not alter receptor expression at the cell surface or internalization. CGRP-stimulated cAMP accumulation was also normal for this mutant (pEC_{50} values: WT 10.54 ± 0.37, W399A 10.10 ± 0.37: Emax W399A 101 ± 8% of WT; basal W399A 5 ± 8% of WT, $n = 3$). Given the likely structural nature of this locus, the wild-type expression of W399A was surprising. Subsequently, three more radical mutants of W399 were made to test the role further. These included a deletion of the residue (W399Del), a threonine substitution (W399T) and a glutamate substitution (W399E). Receptor expression of these three mutants is described in Table 1, with a significant deleterious effect for W399T and almost complete abrogation of expression for W399E.

DISCUSSION

Assigning roles for the C-termini of GPCRs is crucial for understanding the cellular responses of this receptor family. In this study we have established that 12 residues of the proximal C-terminus of CLR, a family B GPCR, are required for cell-surface receptor expression and a discrete peptide mimetic of this region has the potential to form an eighth helix-equivalent of that seen in many family A GPCRs (*13, 39*). The study has also established that a number of residues beyond the eighth helix are required for ligand-induced internalization of the receptor. By contrast, none of the C-terminal tail is needed for coupling to G_s.

The biophysical data and the bioinformatics provide strong evidence that the proximal 12 C-terminal residues of CLR form an eighth helix. While we recognize the possibility that this data may not reflect the native region in CLR, the convergence of both the bioinformatics analysis and the biophysical data strengthens the case that there is an eighth helix in this receptor family.

In the peptide, the conserved distal tryptophan residue (W399) is partially buried in the membrane to anchor the helix. The modified waterLOGSY (SALMON) experiment interestingly suggests insertion into the liposome of protons from opposing sides of the tryptophan side chain of our peptide mimetic. In the intact receptor, a tethered tryptophan may partially fulfill the role of the lipid anchor seen in the equivalent position in the eighth helix in many family A GPCRs, although the family A leukotriene B_4 (BLT1) receptor also has a hydrophobic tether suggested to be a palmitoylation replacement (*14*). However, as the alanine substitution and tryptophan deletion mutants (W399A and W399Del) showed WT-comparable surface expression, this tryptophan does not appear to act alone. The further substitutions of W399 were assessed for surface expression. Replacing the tryptophan for polar residues (W399T and W399E), however, had a significant deleterious effect on expression levels with the more severe effect observed for the charged glutamate residue. These data suggest that while the structural integrity of the tryptophan residue is not an absolute requirement, disruption of this area clearly perturbs trafficking functionality. As the additional three hydrophobic residues V391, L395 and W399 are all aligned on the same side of the helix and are completely conserved in every member of the family B receptors, these may represent the major membrane-interacting residues of the putative eighth helix. In addition, F402, which could be an extension of this structured domain, has the potential to assist with membrane association.

The deletion analysis revealed a specific role for residues 388−400 in promoting cell-surface expression of CLR. Similar effects of disrupted trafficking following the eighth helix mutation have been observed for a variety of family A GPCRs including the V_2R vasopressin receptor and the MC4R muscarinic receptor, although these affect the palmitoylation consensus site (*40*). The residues responsible for the cell surface expression have not yet been delineated; however, the sequence Q/R-x-x-hydrophobic-R/K-K/R is found in 11 out of the 14 receptor sequences examined; the polar residues are all predicted to face the cytosol and seem good candidates for part of a recognition motif.

In some studies, the eighth helix has been considered to play an important part in receptor activation, moving with TM7 (*12–14*). Indeed, the highly conserved E390 would be predicted to be orientated toward the intracellular loops of the TM bundle, where it could potentially interact with conserved basic residues such as R173 at the base of TM2. However, neither the eighth helix nor any other part of the C-terminus was needed for cAMP production. Thus for CLR, while it may have a facilitator role, other residues within the receptor can compensate for the loss of this structure. Of course, independently of any direct effect on coupling, the large decrease in receptor expression seen as a consequence of the helix 8 deletion will cause decreases in both potency and the maximal responses to CGRP for many signaling pathways. However, under the conditions used for this study, the size of the receptor reserve is such that a 90% reduction in expression leads to little change in cAMP production. The impaired internalization shown by Del 400 has at least one functional correlate, as shown by the sustained MAPK response. The data also suggests that the C-terminal tail distal to residue 400 has no impact on MAPK activation, other than via an effect on internalization.

The data on Del 388 has similarities to that reported for the rabbit calcitonin receptor, where removal of the entire C-terminus impaired coupling to G_q, ERK1/2 activation and receptor expression but not G_s coupling (*41*). A similar study using the porcine calcitonin receptor gave broadly consistent results, in that deletion of the entire C-terminus reduced receptor expression, internalization and G_q coupling, but G_s coupling also appeared to be impaired (*42*); either cell-line specific factors or differences in the receptor sequences may explain this discrepancy (Figure 1).

The current study shows that CGRP-mediated internalization requires several dispersed loci distinct from the eighth helix scattered throughout the distal region of the CLR C-terminus. The precise molecular nature of GPCR-internalization is complicated and involves many protein partners; however, serine/threonine phosphorylation is usually a key event and has been demonstrated for CLR (*43*). There is a good correlation between serine/threonine residues in the CLR C-terminus and the degree of internalization (Figure 1; Table 1). By contrast, there are none of the classic dileucine motifs thought to be involved in desensitization (*44*). While internalization is almost completely removed by the absence of the C-terminus after the eighth helix, we have previously shown that the intracellular loop 3 region also has a small but significant effect (*23*). This confirms the disparate nature of residues required for receptor-endocytosis, either forming multiple contacts/phosphorylation sites or having distinct roles in the endocytotic process.

The mechanism of internalization across family B GPCRs shows considerable receptor specificity. Studies of the glucagon-like peptide 2 receptor suggest no role for the C-terminus in ligand-induced desensitization or endocytosis (*19*). There are significant differences with porcine calcitonin receptor (Figure 1b) (*42*). In the latter, an epitope between the equivalent of residues 391 and 418 of CLR was needed for internalization; this has considerable overlap with the main internalization domain identified in the current study; the potential phosphorylation site 411 is conserved in both receptors. However, between the equivalent of residues 419 and 458 was a domain that could impair the actions of the internalization motif; the present study found no evidence for such a motif in CLR. This part of the porcine calcitonin receptor is distinguished by a polyalanine motif, perhaps responsible for masking internalization. Between the equivalent of residue 458 and the end of the C-terminus was a second internalization motif; in combination with the first, this ensured normal receptor internalization. In CLR, residues in this area are also needed for normal internalization.

In summary, this paper has characterized the C-terminus of CLR. Both biochemical and biophysical techniques support the existence for the first time of an eighth helix in a family B GPCR (illustrated in Figure 2), with an important role in cell-surface expression. There is a multiple-residue internalization function contained in a more distal portion of the C-terminus but no part of the structure is needed for coupling to G_s. This study illustrates the power of combining biochemical and biophysical techniques to assign novel structure/function information to this crucial protein family.

ACKNOWLEDGMENT

NMR data were collected at HWB·NMR which is supported by the Wellcome Trust and University of Birmingham. Thanks to Graham Ladds for excellent advice and Corinne Smith for control peptides.

REFERENCES

1. Ostrom, R. S., and Insel, P. A. (2004) The evolving role of lipid rafts and caveolae in G protein-coupled receptor signaling: implications for molecular pharmacology. *Br. J. Pharmacol. 143*, 235–245.
2. Lu, Z. L., Saldanha, J. W., and Hulme, E. C. (2002) Seven-transmembrane receptors: crystals clarify. *Trends Pharmacol. Sci. 23*, 140–146.
3. Bockaert, J., and Pin, J. P. (1999) Molecular tinkering of G protein-coupled receptors: an evolutionary success. *EMBO J. 18*, 1723–1729.
4. Palczewski, K., Kumasaka, T., Hori, T., Behnke, C. A., Motoshima, H., Fox, B. A., Le Trong, I., Teller, D. C., Okada, T., Stenkamp, R. E., Yamamoto, M., and Miyano, M. (2000) Crystal structure of rhodopsin: A G protein-coupled receptor. *Science 289*, 739–745.
5. Schwartz, T. W., Frimurer, T. M., Holst, B., Rosenkilde, M. M., and Elling, C. E. (2006) Molecular mechanism of 7TM receptor activation−a global toggle switch model. *Annu. Rev. Pharmacol. Toxicol. 46*, 481–519.
6. Conner, M., Hawtin, S. R., Simms, J., Wootten, D. L., Lawson, Z., Conner, A. C., Parslow, R. A., and Wheatley, M. (2007) Systematic analysis of the entire second extracellular loop of the V1a vasopressin receptor: Key residues, conserved throughout a G-protein-coupled receptor family, identified. *J. Biol. Chem. 282*, 17405–17412.
7. Cherezov, V., Rosenbaum, D. M., Hanson, M. A., Rasmussen, S. G., Thian, F. S., Kobilka, T. S., Choi, H. J., Kuhn, P., Weis, W. I., Kobilka, B. K., and Stevens, R. C. (2007) High-Resolution Crystal Structure of an Engineered Human {beta}2-Adrenergic G Protein Coupled Receptor. *Science 318*, 1258–1265.
8. Hoare, S. R. (2005) Mechanisms of peptide and nonpeptide ligand binding to Class B G-protein-coupled receptors. *Drug Discovery Today 10*, 417–427.
9. Chen, Z., Gaudreau, R., Le Gouill, C., Rola-Pleszczynski, M., and Stankova, J. (2004) Agonist-induced internalization of leukotriene B(4) receptor 1 requires G-protein-coupled receptor kinase 2 but not arrestins. *Mol. Pharmacol. 66*, 377–386.
10. Piserchio, A., Zelesky, V., Yu, J., Taylor, L., Polgar, P., and Mierke, D. F. (2005) Bradykinin B2 receptor signaling: structural and functional characterization of the C-terminus. *Biopolymers 80*, 367–373.
11. Schoneberg, T., Schulz, A., Biebermann, H., Hermsdorf, T., Rompler, H., and Sangkuhl, K. (2004) Mutant G-protein-coupled receptors as a cause of human diseases. *Pharmacol. Ther. 104*, 173–206.
12. Tao, Y. X. (2006) Inactivating mutations of G protein-coupled receptors and diseases: structure-function insights and therapeutic implications. *Pharmacol. Ther. 111*, 949–973.
13. Choi, G., Guo, J., and Makriyannis, A. (2005) The conformation of the cytoplasmic helix 8 of the CB1 cannabinoid receptor using NMR and circular dichroism. *Biochim. Biophys. Acta 1668*, 1–9.
14. Okuno, T., Ago, H., Terawaki, K., Miyano, M., Shimizu, T., and Yokomizo, T. (2003) Helix 8 of the leukotriene B4 receptor is required for the conformational change to the low affinity state after G-protein activation. *J. Biol. Chem. 278*, 41500–41509.
15. Marin, E. P., Krishna, A. G., Zvyaga, T. A., Isele, J., Siebert, F., and Sakmar, T. P. (2000) The amino terminus of the fourth cytoplasmic loop of rhodopsin modulates rhodopsin-transducin interaction. *J. Biol. Chem. 275*, 1930–1936.
16. Mukhopadhyay, S., Cowsik, S. M., Lynn, A. M., Welsh, W. J., and Howlett, A. C. (1999) Regulation of Gi by the CB1 cannabinoid receptor C-terminal juxtamembrane region: structural requirements determined by peptide analysis. *Biochemistry 38*, 3447–3455.
17. Mukhopadhyay, S., McIntosh, H. H., Houston, D. B., and Howlett, A. C. (2000) The CB(1) cannabinoid receptor juxtamembrane C-terminal peptide confers activation to specific G proteins in brain. *Mol. Pharmacol. 57*, 162–170.
18. Tetsuka, M., Saito, Y., Imai, K., Doi, H., and Maruyama, K. (2004) The basic residues in the membrane-proximal C-terminal tail of the rat melanin-concentrating hormone receptor 1 are required for receptor function. *Endocrinology 145*, 3712–3723.
19. Estall, J. L., Koehler, J. A., Yusta, B., and Drucker, D. J. (2005) The glucagon-like peptide-2 receptor C terminus modulates beta-arrestin-2 association but is dispensable for ligand-induced desensitization, endocytosis, and G-protein-dependent effector activation. *J. Biol. Chem. 280*, 22124–22134.
20. Langlet, C., Langer, I., Vertongen, P., Gaspard, N., Vanderwinden, J. M., and Robberecht, P. (2005) Contribution of the carboxyl terminus of the VPAC1 receptor to agonist-induced receptor phosphorylation, internalization, and recycling. *J. Biol. Chem. 280*, 28034–28043.
21. Seck, T., Baron, R., and Horne, W. C. (2003) Binding of filamin to the C-terminal tail of the calcitonin receptor controls recycling. *J. Biol. Chem. 278*, 10408–10416.
22. Conner, A. C., Hay, D. L., Simms, J., Howitt, S. G., Schindler, M., Smith, D. M., Wheatley, M., and Poyner, D. R. (2005) A key role for transmembrane prolines in calcitonin receptor-like receptor agonist binding and signalling: implications for family B G-protein-coupled receptors. *Mol. Pharmacol. 67*, 20–31.
23. Conner, A. C., Simms, J., Conner, M. T., Wootten, D. L., Wheatley, M., and Poyner, D. R. (2006) Diverse functional motifs within the three intracellular loops of the CGRP1 receptor. *Biochemistry 45*, 12976–12985.
24. Conner, A. C., Simms, J., Howitt, S. G., Wheatley, M., and Poyner, D. R. (2006) The second intracellular loop of the calcitonin gene-related peptide receptor provides molecular determinants for signal transduction and cell surface expression. *J. Biol. Chem. 281*, 1644–1651.
25. McLatchie, L. M., Fraser, N. J., Main, M. J., Wise, A., Brown, J., Thompson, N., Solari, R., Lee, M. G., and Foord, S. M. (1998) RAMPs regulate the transport and ligand specificity of the calcitonin-receptor-like receptor. *Nature 393*, 333–339.
26. Poyner, D. R., Andrew, D. P., Brown, D., Bose, C., and Hanley, M. R. (1992) Pharmacological characterization of a receptor for calcitonin gene-related peptide on rat, L6 myocytes. *Br. J. Pharmacol. 105*, 441–447.
27. Plevin, R., Scott, P. H., Robinson, C. J., and Gould, G. W. (1996) Efficacy of agonist-stimulated MEK activation determines the susceptibility of mitogen-activated protein (MAP) kinase to inhibition in rat aortic smooth muscle cells. *Biochem. J. 318*, 657–663. (Part 2).
28. San Miguel, M., Marrington, R., Rodger, P. M., Rodger, A., and Robinson, C. (2003) An Escherichia coli twin-arginine signal peptide switches between helical and unstructured conformations depending on the hydrophobicity of the environment. *Eur. J. Biochem./FEBS 270*, 3345–3352.
29. Woody, R. W. (1994) Contributions of tryptophan side chains to the far-ultraviolet circular dichroism of proteins. *Eur. Biophys. J. 23*, 253–262.
30. Dalvit, C., Pevarello, P., Tato, M., Veronesi, M., Vulpetti, A., and Sundstrom, M. (2000) Identification of compounds with binding affinity to proteins via magnetization transfer from bulk water. *J. Biomol. NMR 18*, 65–68.
31. Ludwig, C., Michiels, P. J., Wu, X., Kavanagh, K. L., Pilka, E., Jansson, A., Oppermann, U., and Günther, U. L. (2007) SALMON: Solvent Accessibility, Ligand binding and Mapping of ligand Orientation by NMR spectroscopy. *J. Med. Chem. 51*, 1–3.
32. Jaysinghe, S., Hristova, K., Wimley, W., Snider, C., and White, S. (2006)http://blanco.biomol.uci.edu/mpex.
33. Eisenberg, D., Weiss, R. M., and Terwilliger, T. C. (1982) The helical hydrophobic moment: a measure of the amphiphilicity of a helix. *Nature 299*, 371–374.
34. Wallace, J., Daman, O. A., Harris, F., and Phoenix, D. A. (2004) Investigation of hydrophobic moment and hydrophobicity properties for transmembrane alpha-helices. *Theor. Biol. Med. Modell. 1*, 5.
35. Jasanoff, A., and Fersht, A. R. (1994) Quantitative determination of helical propensities from trifluoroethanol titration curves. *Biochemistry 33*, 2129–2135.
36. Dafforn, T. a. R. A. (2004) Linear dichroism of biomolecules: which way is up. *Curr. Opin. Struct. Biol. 14*, 541–546.
37. Rajendra, J. D. A., Hicks, M., Booth, P., Rodger, P. M., and Rodger, A. (2006) Quantitation of protein orientation in flow-oriented unilamellar liposomes by linear dichroism. *Chem. Phys. 326*, 210–220.
38. Lacowicz, J. R. (1986) *Principles of fluorescence spectroscopy*, Plenum Press, New York.

39. Katragadda, M., Maciejewski, M. W., and Yeagle, P. L. (2004) Structural studies of the putative helix 8 in the human beta(2) adrenergic receptor: an NMR study. *Biochim. Biophys. Acta 1663*, 74–81.
40. Tobin, A. B., and Wheatley, M. (2004) G-protein-coupled receptor phosphorylation and palmitoylation. *Methods Mol. Biol. 259*, 275–281.
41. Seck, T., Pellegrini, M., Florea, A. M., Grignoux, V., Baron, R., Mierke, D. F., and Horne, W. C. (2005) The delta e13 isoform of the calcitonin receptor forms a six-transmembrane domain receptor with dominant-negative effects on receptor surface expression and signaling. *Mol. Endocrinol. 19*, 2132–2144.
42. Findlay, D. M., Houssami, S., Lin, H. Y., Myers, D. E., Brady, C. L., Darcy, P. K., Ikeda, K., Martin, T. J., and Sexton, P. M. (1994) Truncation of the porcine calcitonin receptor cytoplasmic tail inhibits internalization and signal transduction but increases receptor affinity. *Mol. Endocrinol. 8*, 1691–1700.
43. Hilairet, S., Belanger, C., Bertrand, J., Laperriere, A., Foord, S. M., and Bouvier, M. (2001) Agonist-promoted internalization of a ternary complex between calcitonin receptor-like receptor, receptor activity-modifying protein 1 (RAMP1), and beta-arrestin. *J. Biol. Chem. 276*, 42182–42190.
44. Gaudreau, R., Beaulieu, M. E., Chen, Z., Le Gouill, C., Lavigne, P., Stankova, J., and Rola-Pleszczynski, M. (2004) Structural determinants regulating expression of the high affinity leukotriene B4 receptor: involvement of dileucine motifs and α helix VIII. *J. Biol. Chem. 279*, 10338–10345.

BI8004126